Supporting Information for

Molecular chains of coordinated dimolybdenum isonicotinate paddlewheel clusters

Minyuan M. Li,[a,b,^] F. James Claire,[a,^] Marina A. Solomos,[a,^] Stephanie M. Tenney,[a,c] Sergei A. Ivanov,[b] Maxime A. Siegler,[a] Thomas J. Kempa [a,d,*]

[a] Department of Chemistry, The Johns Hopkins University, Baltimore, MD 21218, United States

[b] Center for Integrated Nanotechnologies, Los Alamos National Laboratory, PO Box 5800, MS 1315; Albuquerque, NM 87185, United States

[c] Current address: Department of Chemistry and Biochemistry, University of California, Los Angeles, 607 Charles E. Young Drive East, Los Angeles, CA 90095, United States

[d] Department of Materials Science and Engineering, The Johns Hopkins University, Baltimore, MD 21218, United States

^ These authors contributed equally

* Corresponding author: tkempa@jhu.edu

Materials and Methods:

All glassware was cleaned and oven-dried prior to usage. All solvents were thoroughly degassed under inert atmosphere (N_2). Schlenk line techniques were used in the syntheses of molybdenum (II) acetate and molybdenum (II) isonicotinate.

1. Synthesis of Molybdenum (II) Acetate ($Mo_2(O_2CCH_3)_4$)[1,2]

A 500-mL round-bottom flask was charged with molybdenum hexacarbonyl (3.0 g, 11 mmol). To this flask, acetic acid (100 mL), acetic anhydride (20 mL), and hexane (5 mL) were added. The solution was refluxed at 130 °C for 20 hours with stirring. The solution turned brown, and a bright yellow crystalline solid precipitated. The yellow solid was filtered under N_2 and washed with ethanol. The product was dried under vacuum and stored under N_2 at −20 °C. Yield: 37.1%

2. Synthesis of product 1

A solution of $Mo_2(O_2CCH_3)_4$ (0.250 g, 0.584 mmol) and isonicotinic acid (0.712 g, 5.79 mmol) in 50 mL anhydrous dimethylformamide (DMF) was prepared in a 100-mL Schlenk flask under an N_2 atmosphere. To this solution, a trace amount of acetic acid (0.033 mL, 0.574 mmol) was added. The red solution was refluxed at 120 °C for two days while stirring at 300 rpm. The resulting bright red product **1** was filtered under N_2, washed with DMF, and dried under vacuum. The product was stored under N_2. Yield: 62%. Elemental analysis measures 42.28% C, 3.00% H, 9.12% N, and 25.74% Mo (theoretical values: 43.04% C, 3.08% H, 9.30% N, and 25.47% Mo). When this reaction is performed with a stirring speed of 60 rpm, single crystals large enough for x-ray diffraction studies are deposited on the sidewalls of the flask.

3. Mass spectroscopy

A solution of **1** (5 mg) in 2 mL dimethylsulfoxide (DMSO) was diluted in 20 mL of acetonitrile. This solution was analyzed in positive mode ESI-MS on a Thermo Finnigan LCQ Duo Ion Trap Mass Spectrometer.

4. Single crystal XRD

All reflection intensities were measured at 110(2) K using a SuperNova diffractometer (equipped with Atlas detector) with Mo Kα radiation (λ = 0.71073 Å) under the program CrysAlisPro (Version CrysAlisPro 1.171.39.29c, Rigaku OD, 2017). The same program was used to refine the cell dimensions and for data reduction. The structure was solved with the program SHELXS-2014/7 and was refined on F2 with SHELXL-2014/7.[3] A numerical absorption correction based on Gaussian integration over a multifaceted crystal model was applied using CrysAlisPro. The temperature of the data collection was controlled using the system Cryojet (manufactured by Oxford Instruments). The H atoms were placed at calculated positions (unless otherwise specified) using the instructions AFIX 33, AFIX 43 or

AFIX 137 with isotropic displacement parameters having values 1.2 or 1.5 Ueq of the attached C atoms. The structure is partly disordered.

Both Mo1-Mo1 and Mo2-Mo2 complexes are found at sites of inversion symmetry, and only the halves are crystallographically independent. The DMF molecules coordinated to the Mo2-Mo2 complex and one of the pyridine rings are disordered over two orientations. The occupancy factors of the major components of the disorder refine to 0.942(3) and 0.52(3), respectively.

5. NMR of 1 after acid digestion

^{1}H NMR spectra were obtained on a Bruker Avance 400 MHz spectrometer. Samples were prepared by dissolving approximately 5 mg of vacuum-dried **1** in 500 μL DMSO-d_6 and 100 μL dilute DCl solution (23 μL 35% DCl in D_2O, diluted in 1.0 mL DMSO).

6. Powder X-ray diffraction

Powder X-ray diffraction data were collected on a Bruker D8 Focus diffractometer using a Cu X-ray source (Kα = 8.04 keV, 1.5406 Å). The simulated pXRD pattern was calculated using the Mercury 3.10 powder calculation function. The simulated wavelength was set to 1.54056 Å and the peak shape was calculated for a FWHM (2θ) equal to 0.1.

7. Raman Spectroscopy

Raman spectroscopy was performed on a Horiba-Jobin-Yvon T64000 Raman Spectrometer using a 514 nm laser at 1 mW. The spectrum was collected on **1** with a 1800 grooves/mm grating during a 30 s exposure.

8. Infrared Spectroscopy

Infrared spectroscopy was performed on **1** with a ThermoNicolet Nexus 670 FTIR Spectrometer using OMNIC 6.0a operating software.

9. BET Analysis

Gas adsorption analysis was conducted on an ASAP 2020 V4.04 using N_2 as the adsorbate gas at 77.417 K. Measurements were made on 0.0797 g of **1** that was degassed overnight at 90 °C until vacuum stabilized at 10 μmHg. Partial pressures during the measurement ranged between 0.0067 p/p_0 to 0.5500 p/p_0 in a flask with 85.9091 cm^3 cold free space.

10. Thermogravimetric Analysis

Thermogravimetric analysis was performed on a SDT Q600 (V20.9 Build 20) instrument using alumina pans. Measurements were made from room temperature to 700 °C at a ramp rate of 5 °C/min under a nitrogen flush of 100 mL/min. A sample of **1** (3.6432 mg) was prepared by drying under vacuum, at room temperature, for 48 hours prior to TGA measurement.

11. Electron Paramagnetic Resonance

Electron paramagnetic resonance spectroscopy was performed using a Bruker EPR spectrometer with an ER 073 10" magnet and a Bruker ER041 XG microwave bridge. Measurements were made on a powder sample of **1** in a 4.0 mm quartz tube at 20 K using X-band microwave frequency (9.442639 GHz).

Simulation of the field-sweep continuous wave EPR spectrum was performed in EasySpin 5.2.20 in the slow-motional regime with axial symmetry from the following parameters under Sys: S = ½; Nucs = '(95,96,97)Mo'; Abund = [0.16 0.74 0.1]; g = [1.9345 1.8950]; A = [110 20], lw = 3, and tcorr = 1e-8. The system exhibits better fits under axial symmetry rather than under isotropic or rhombic symmetry.

12. Absorption Spectroscopy

Solid-state UV-vis absorption spectroscopy was performed on powder of **1** on glass using a Cary 5000 UV-Vis-NIR Spectrophotometer from Agilent Technologies with an integrating sphere.

Absorption spectroscopy on solutions was performed on a Cary 60 UV-Vis Spectrophotometer from Agilent Technologies. A solution of $Mo_2(INA)_4$ in DMF was prepared by letting 5 mg of **1** powder sit in 5 mL dry DMF at room temperature and then removing the supernatant for measurement.

13. Elemental Analysis

Elemental analysis was performed at Robertson Microlit Laboratories.

14. DFT Calculations

Computational resources were provided by the Maryland Advanced Research Computing Center (MARCC). Time-dependent DFT (TD-DFT) and molecular orbital calculations were completed using Gaussian09. The B3LYP functional was used along with a split basis set (6-31g* for H, C, N, O atoms and SDD for Mo atoms). Since the XYZ coordinates of 1 were obtained directly from the cif of the compound, single point energies were calculated. Avogadro 1.2.0 was used to isolate XYZ coordinates of the monomer. The same method produced XYZ coordinates the dimer. TD-DFT electronic absorptions were analyzed and visualized using GaussView 5.0.9. Molecular orbitals were rendered in Chemcraft 1.8.

Figure S1

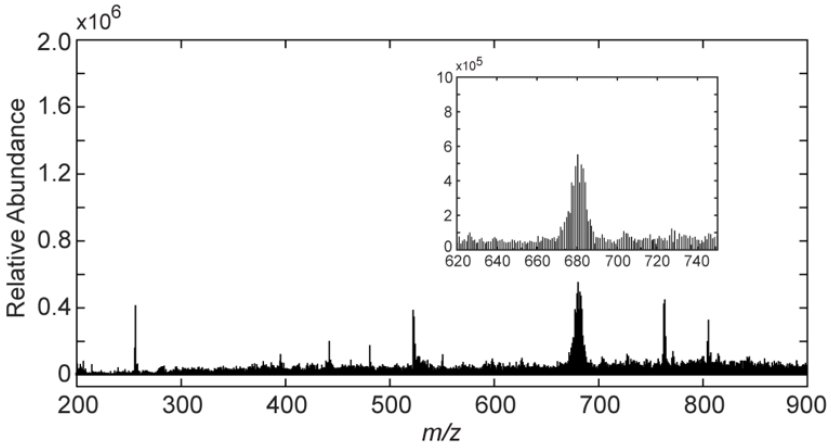

Figure S1. The mass spectrum of **1** as a solution in DMSO/ACN reveals a cluster of peaks centered at a molecular ion of 681 m/z. A distribution of peaks about this value is anticipated due to the relative abundance of several isotopes associated with the atoms within the $Mo_2(INA)_4$ cluster.

Figure S2

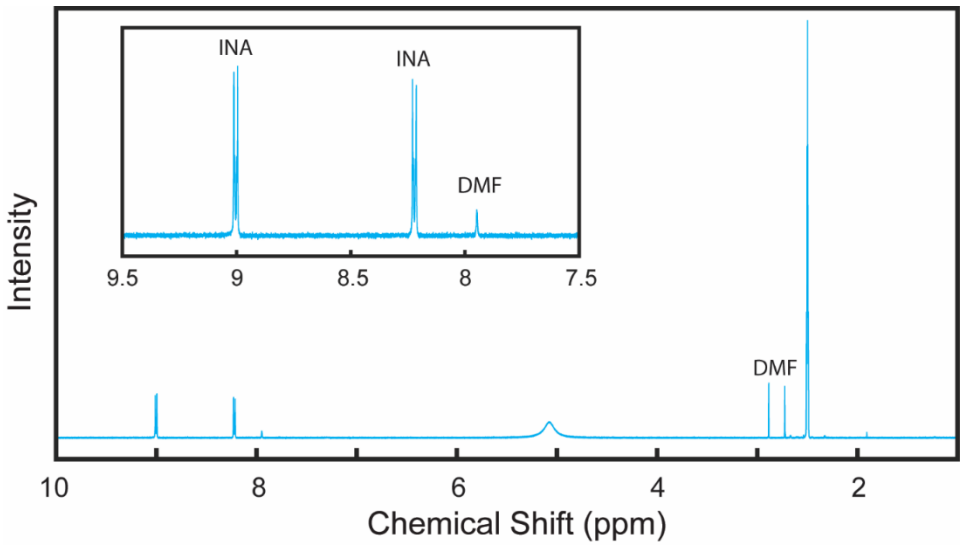

Figure S2. ^{1}H NMR spectrum of 1 after acid digestion. There is one coordinated DMF molecule per $Mo_2(INA)_4$ cluster unit after digestion of **1** in acid. In the ^{1}H NMR spectrum, three singlet peaks are observed for the coordinated DMF molecules: δ 7.95 ppm, 1H, integrated to 1.00; δ 2.89 ppm, 3H, integrated to 3.27; δ 2.73 ppm, 3H, integrated to 3.26. Two unique aromatic hydrogen atoms are observed in the INA ligands (δ 9.00 ppm, 2H, d, integrated to 8.14; δ 8.22 ppm, 2H**,** d, integrated to 8.13). The ratio of DMF to INA is approximately 1 to 4.07. Peaks for water and DMSO are observed at 5.08 ppm and 2.50 ppm, respectively.

Figure S3

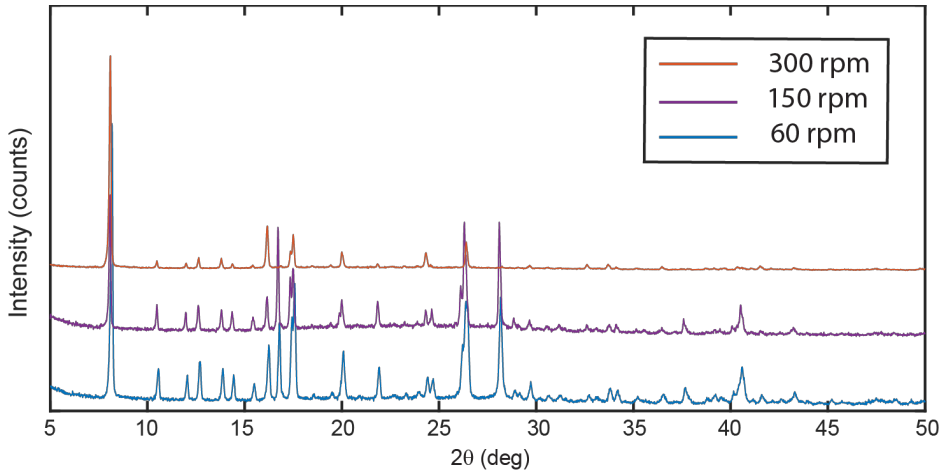

Figure S3. Powder X-ray diffraction scans of 1 synthesized at various reaction stir rates. The synthesis of **1** was performed at various reaction stir rates to determine the effect of solution agitation on crystal structure of the crystalline powder product. When the reaction is performed at 300 rpm, all of the product recovered is in polycrystalline powder form. At 60 rpm, the reaction produces large single crystals as well as powder product.

Table S1

Crystallographic data:

Crystal data	
Chemical formula	$C_{27}H_{23}Mo_2N_5O_9$
M_r	753.38
Crystal system, space group	Triclinic, *P*-1
Temperature (K)	110
a, *b*, *c* (Å)	8.5571 (3), 11.9579 (5), 15.1881 (5)
α, β, γ (°)	111.799 (3), 92.248 (3), 99.262 (3)
V (Å^3)	1415.84 (10)
Z	2
Radiation type	Mo *K*α
μ (mm^{-1})	0.95
Crystal size (mm)	0.12 × 0.05 × 0.03
Data collection	
Diffractometer	SuperNova, Dual, Cu at zero, Atlas
Absorption correction	Gaussian *CrysAlis PRO* 1.171.39.29c (Rigaku Oxford Diffraction, 2017) Numerical absorption correction based on gaussian integration over a multifaceted crystal model Empirical absorption correction using spherical harmonics, implemented in SCALE3 ABSPACK scaling algorithm.
T_{min}, T_{max}	0.890, 1.000
No. of measured, independent and observed [$I > 2\sigma(I)$] reflections	21519, 6499, 5123
R_{int}	0.042
$(\sin \theta/\lambda)_{max}$ (Å^{-1})	0.650
Refinement	
$R[F^2 > 2\sigma(F^2)]$, $wR(F^2)$, *S*	0.033, 0.062, 1.06

No. of reflections	6499
No. of parameters	461
No. of restraints	350
H-atom treatment	H-atom parameters constrained
$\Delta\rho_{max}$, $\Delta\rho_{min}$ (e Å^{-3})	0.53, -0.47

Figure S4

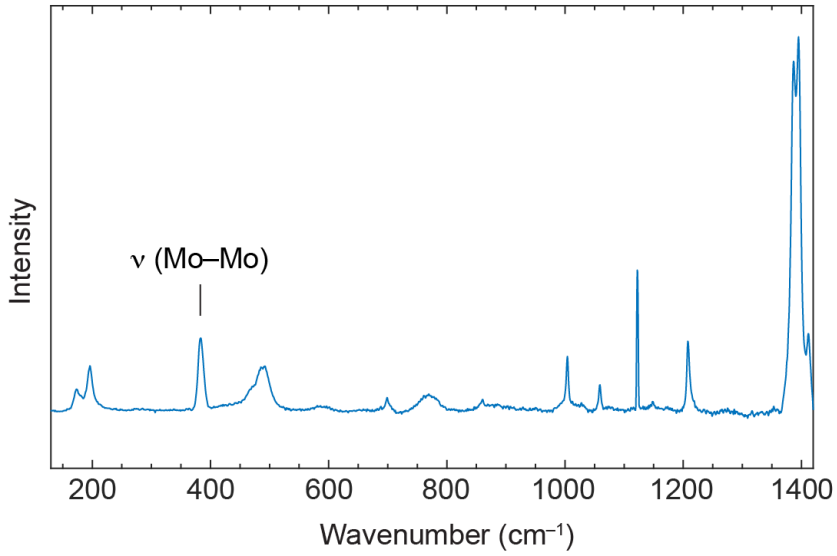

Figure S4. Raman spectrum of 1. The band at 383 cm^{-1} is assigned to the dimolybdenum symmetric mode, and is within the range of values reported in the literature.[4]

Figure S5

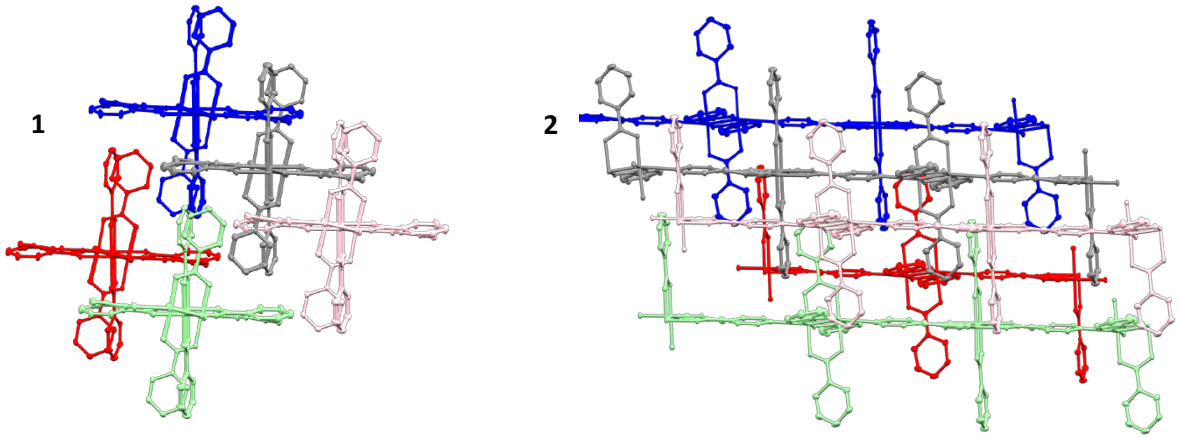

Figure S5. Crystal packing of 1. Packing of the one-dimensional coordination polymers down the axis of coordination (View 1), and along the sides of the 1D molecular chains (View 2).

Figure S6

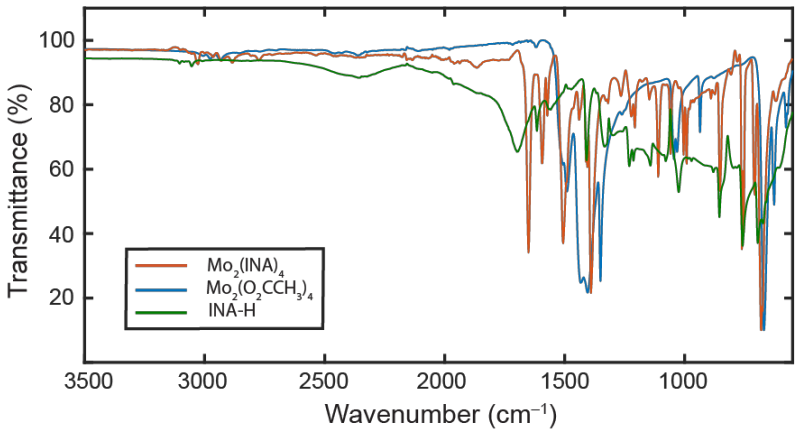

Figure S6. Infrared spectra. Starting materials (isonicotinic acid, green; molybdenum tetraacetate, blue) and **1** (red) after reaction at a stir rate of 300 rpm.

Figure S7

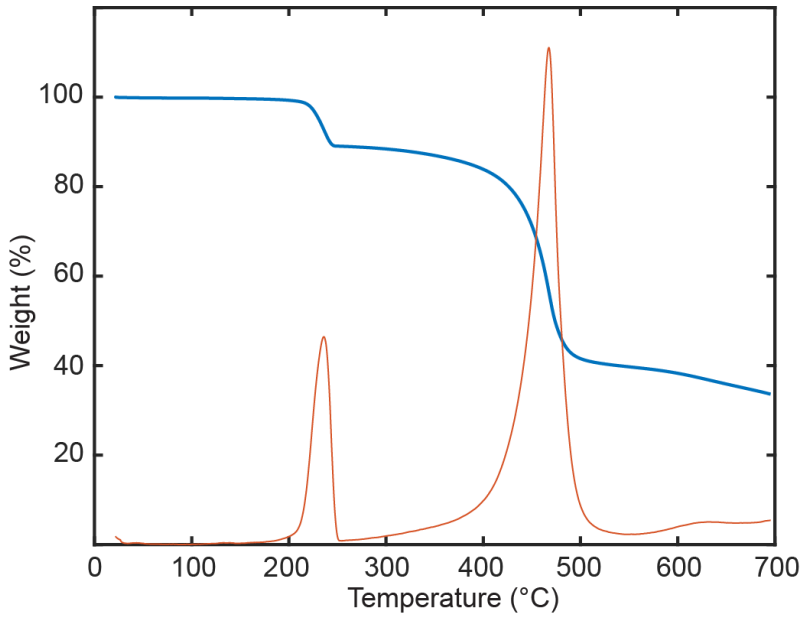

Figure S7. Thermogravimetric analysis of 1. The weight loss curve (blue) and its derivative (orange) show a sharp mass loss of 10.1 % between 190 °C and 252 °C, which likely corresponds to the loss of coordinated DMF (9.7 %). The coordination polymer began to rapidly lose mass above 350 °C, a likely sign of degradation.

Figure S8

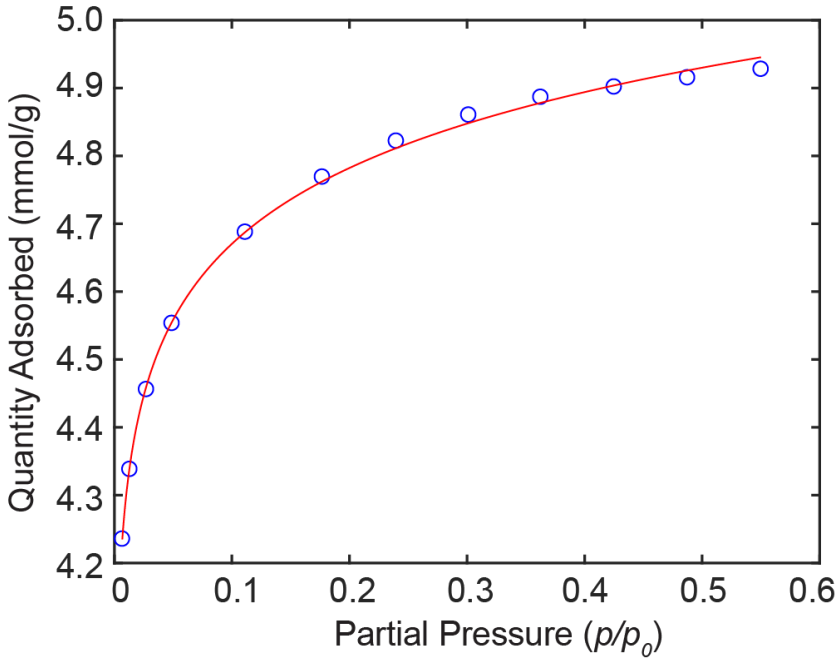

Figure S8. N_2 adsorption isotherm of 1. The N_2 adsorption isotherm for **1** collected at 77 K. The fit (red line) to the data was used to calculate an apparent BET surface area of 325.8 m^2/g.

Figure S9

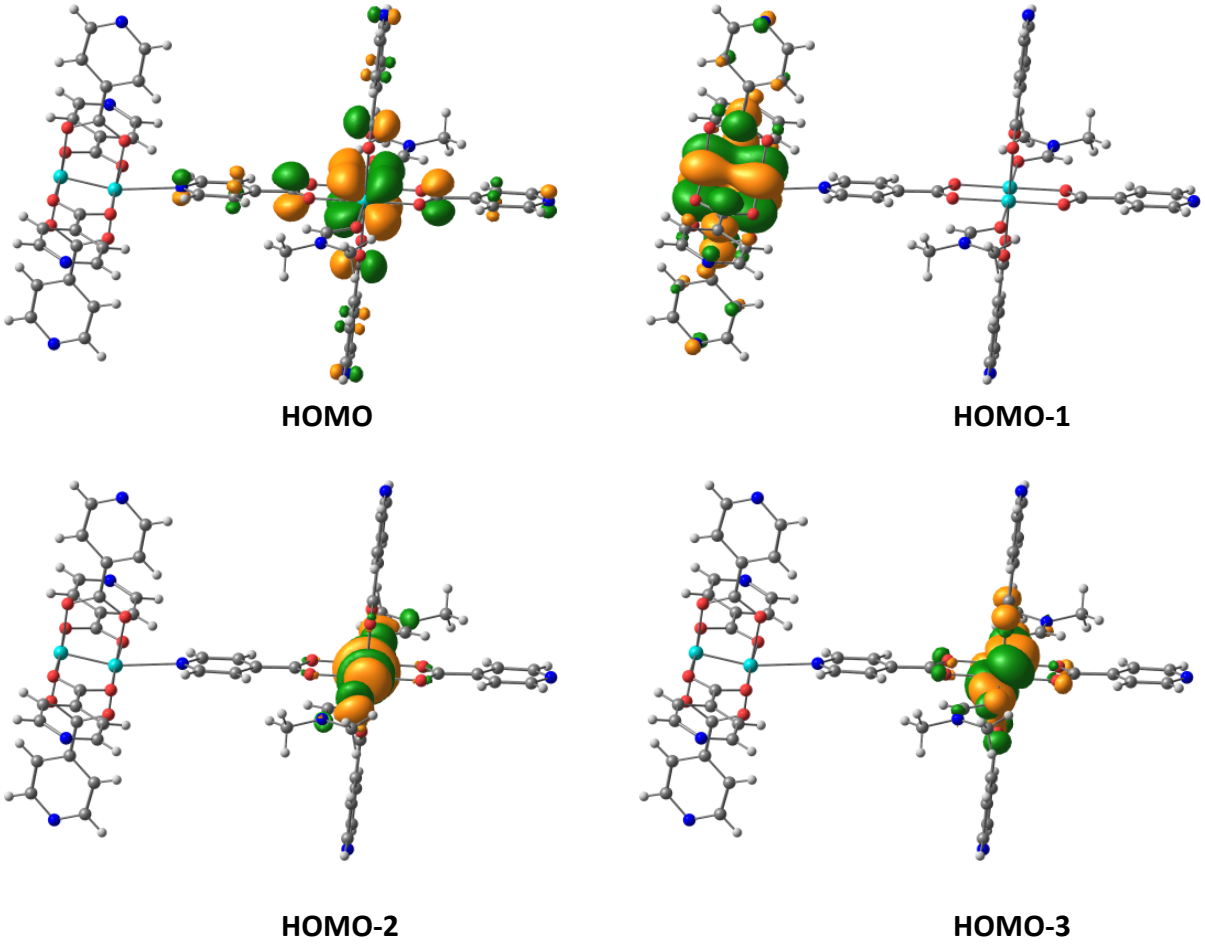

Figure S9. Electron densities from highest occupied molecular orbitals of the dimer. Four highest occupied molecular orbitals from single-point energy calculations on the dimer, showing localized and metal-centered electron densities.

Figure S10

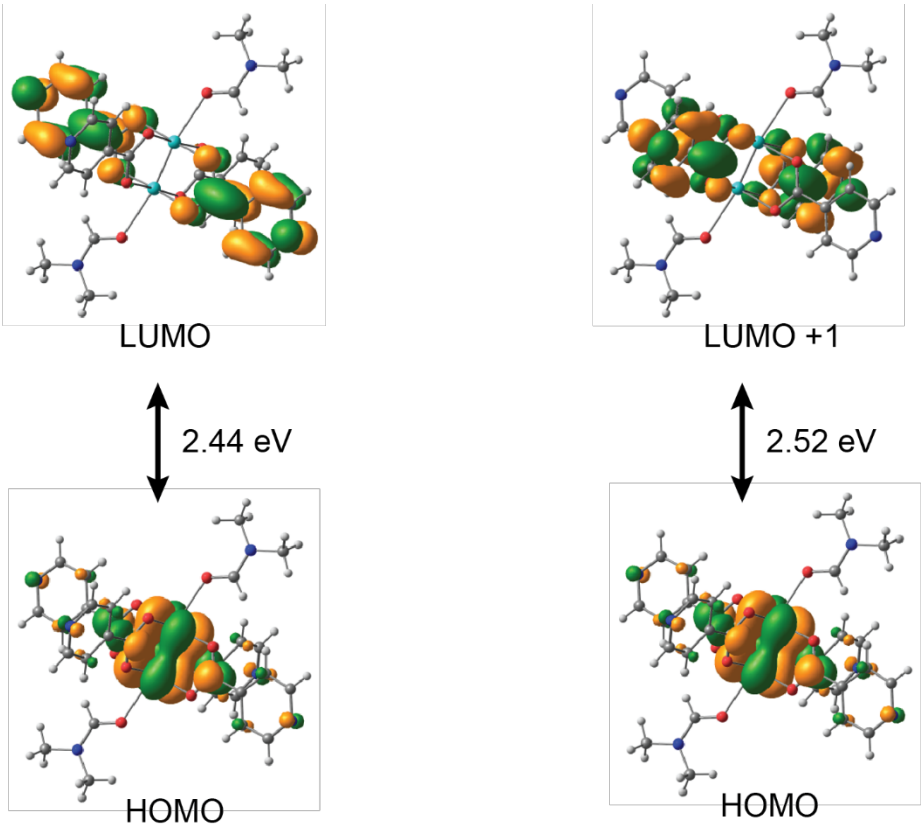

Figure S10. Calculated electronic transitions of the monomer. There are two main electronic transitions calculated for a single paddlewheel unit coordinated to DMF. Both occur primarily between δ(Mo_2) orbitals (HOMO) and ligand π* orbitals (LUMO and LUMO +1).

Figure S11

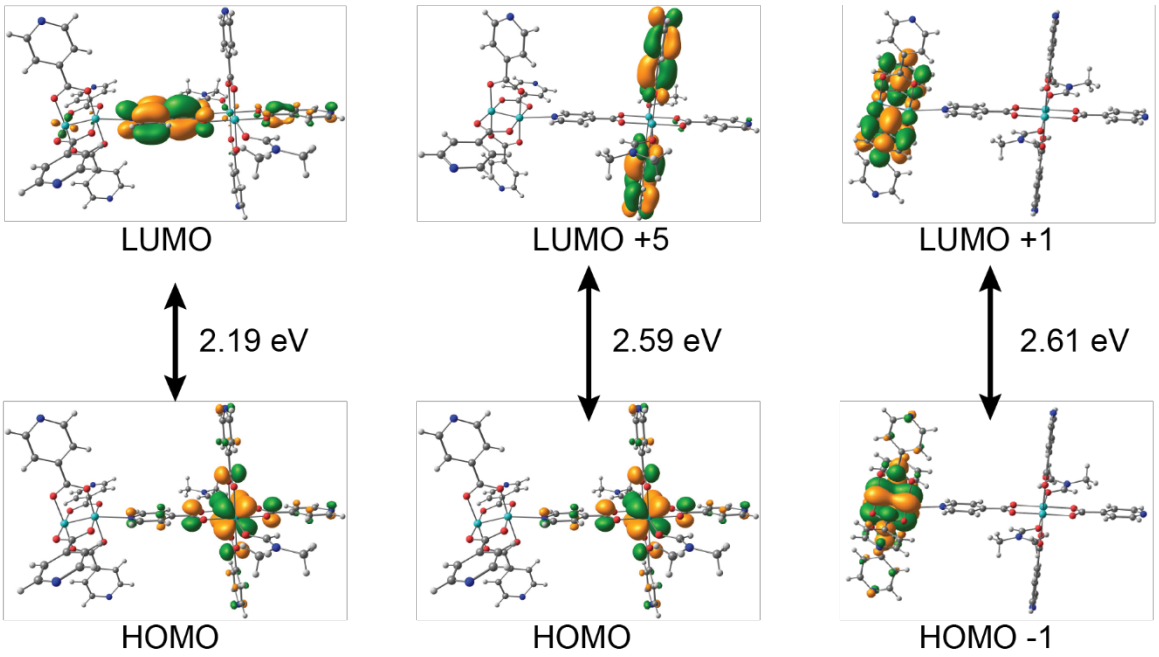

Figure S11. Calculated electronic transitions of the dimer. Three electronic transitions were calculated to be major contributors in the absorbance spectrum based on the calculations of a representative dimer. The HOMO-LUMO transition (2.19 eV, 566 nm) occurs primarily from the $\delta(Mo_2)$ orbital of the DMF-coordinated paddlewheel to the π^* of the INA ligand connecting the two paddlewheels, along the direction of the one-dimensional chain. Another major transition (2.59 eV, 479 nm) comes primarily from the HOMO $\delta(Mo_2)$ to the π^* (LUMO +5) of the ligands perpendicular to the connecting ligand. A similar transition (2.61 eV, 475 nm) occurs at the $\delta(Mo_2)$ orbital of the paddlewheel not coordinated to DMF (HOMO -1) to the attached ligand π^* (LUMO +1). The two higher energy transitions are perpendicular to the direction of the one-dimensional chain.

Figure S12

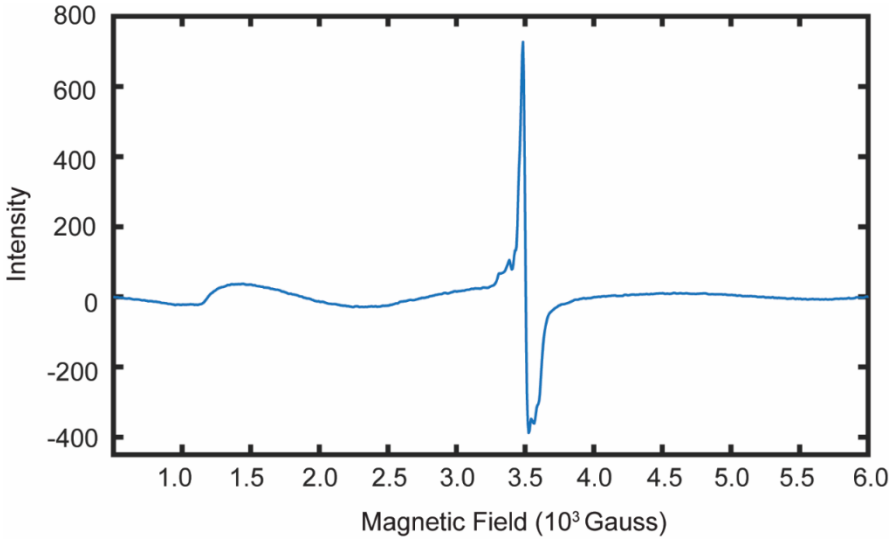

Figure S12. Electron paramagnetic resonance spectrum of 1. The system was modeled as an axial paramagnet.[5] Hyperfine splitting due to molybdenum isotopes (^{95}Mo, I = 5/2; ^{97}Mo, I = 5/2) was observed with a coupling constant of 3.9 mT. A broad feature was also observed around 1500 G (g ~ 4.5) and may be attributed to impurities or forbidden half-field transitions.[6]

References:

1. T. A. Stephenson, E. Bannister and G. Wilkinson, *J. Chem. Soc.*, 1964, **0**, 2538.
2. L. E. Pence, A. M. Weisgerber and F. A. Maounis, *J. Chem. Educ.*, 1999, **76**, 404.
3. Sheldrick, G. M. SHELXTL Version 2014/7. http://shelx.uni-ac.gwdg.de/SHELX/index.php
4. F. A. Cotton and J. G. Norman, *J. Am. Chem. Soc.*, 1972, **94**, 5697–5702.
5. F.E. Mabbs, and D. Collison, *Electron Paramagnetic Resonance of d Transition Metal Compounds,* Elsiever Science Publishers, Amsterdam, The Netherlands, 1992
6. F. A. Cotton, N. S. Dalal, C. Y. Liu, C. A. Murillo, J. M. North and X. Wang, *J. Am. Chem. Soc.*, 2003, **125**, 12945–12952.